JOURNAL OF APPLIED ELECTROCHEMISTRY 14 (1984) 107–115

Plasma-sprayed nickel cathode coatings for hydrogen evolution in alkaline electrolytes

D. E. HALL

Inco Alloy Products Company Research Center, Inco–Sterling Forest, Suffern, New York 10901, USA

Received 6 April 1983

Hydrogen evolution cathodes with plasma-sprayed nickel coatings were much more efficient in alkaline electrolytes than either uncoated cathodes or cathodes with porous sintered nickel coatings. This efficiency improvement could not be attributed to either superior coating morphology or increased surface area. The degree of coating oxidation appeared to be the main factor influencing the hydrogen evolution overpotentials at either the plasma-sprayed or sintered nickel cathode coatings studied. Highly-oxidized nickel surfaces produced much lower Tafel slopes than similar unoxidized surfaces. Plasma-sprayed nickel cathode coatings made with fine, high surface area nickel powder produced hydrogen evolution overpotentials in the range 0.10–0.14 V.

1. Introduction

In recent years there has been considerable research on hydrogen evolution cathodes for alkaline electrochemical systems. The major application for such cathodes is in the chlor-alkali industry, where the high hydrogen evolution overpotentials of present cathodes contribute significantly to cell energy losses. More efficient hydrogen evolution cathodes are also needed for alkaline water electrolysis, in which hydrogen is the primary product. Today's hydrogen evolution cathodes are generally made of steel or nickel. To compete economically, new cathodes will have to be relatively inexpensive as well as more energy-efficient. Thus, much of the recent work to improve cathode efficiency has involved coating steel or nickel cathode substrates with base metals and their alloys and intermetallic compounds.

Among the coating methods which have been investigated, plasma-spraying has been studied as a means of reducing cathode overpotential by increasing the cathode surface area, taking advantage of the surface roughness produced by the spraying process [1]. The method has also been used as a convenient way of depositing nickel–aluminium coatings, which can then be leached to give Raney nickel cathode surfaces [2, 3]; other metals with desirable electrocatalytic properties, such as molybdenum, can be codeposited. A recent patent [4] disclosed a plasma-sprayed cathode coating in which the metal powder was codeposited with an inorganic salt. Leaching the salt with water produced a cathode coating with higher porosity than can be obtained by spraying only metal powder.

Recently, Yoshida and Shiroki [5] showed that the high efficiency of plasma-sprayed nickel cathode coatings was related to thermal oxidation of the coating material resulting from the spray-coating process. We report here an independent study of plasma-sprayed nickel cathode coatings in which physical and chemical differences between coatings made with various nickel powders are described. These characteristics are then related to corresponding differences in hydrogen evolution overpotentials. The relatively high efficiencies of the plasma-sprayed nickel cathode coatings are compared with other types of nickel cathode coatings. Similarities and differences between Yoshida and Shiroki's study [5] and the present work are discussed.

2. Experimental details

2.1. *Cathode preparation*

Plasma-sprayed nickel cathode coatings were pre-

0021-891X/84 $03.00 + .12.

pared using a METCO* 7M plasma spray unit. The coatings were deposited on sandblasted steel sheets and discs, and on etched steel screens. Coatings were made from INCO† Type 123 nickel powder ('Ni 123' below), and METCO 56F-NS and 56C-NS nickel powders. For comparison, other types of cathodes were also prepared. These included uncoated, sandblasted steel sheets and cathodes made by sintering porous nickel coatings onto mild steel sheets. The preparation of the latter type is described in detail elsewhere [6]. Test cathodes were made from the sheet and screen materials by cutting them to appropriate size and tack-welding a nickel wire to each. The wire was insulated with epoxy resin. The back and edges of each sheet cathode were also insulated, with epoxy lapped over the front (test) face of the sheet, to give a geometric surface area of approximately 7 cm^2 for each finished cathode. The disc cathodes were tested in a PTFE test cell [7] in which the active surface area of each cathode was restricted to 5.7 cm^2 by an *o*-ring seal.

To clarify the effect of thermal oxidation of the plasma-sprayed cathode coatings on their hydrogen evolution efficiencies, some cathodes were reduced under flowing hydrogen after spray coating. Both sheet and screen cathodes with Ni 123 coatings were reduced for 30 min at temperatures from 200 to 500° C. The cathodes were furnace-cooled under the hydrogen atmosphere until room temperature was reached. Additionally, some cathodes with porous sintered nickel coatings were thermally oxidized under air at temperatures ranging from 350 to 725° C.

Some plasma-sprayed Ni 123 cathode coatings were impregnated with $Ni(OH)_2$ to investigate reducing their hydrogen evolution overpotentials in this way, as reported [8] with other types of nickel cathodes. $Ni(OH)_2$ impregnation was carried out using the cathodic precipitation process described by McHenry [9]. A cathode current density of 7 mA cm^{-2} was applied in aqueous 0.2 mol dm^{-3} $Ni(NO_3)_2$ at 50° C. Different $Ni(OH)_2$ loadings, determined by weight gain measurements, were achieved by varying the time during which current was passed.

* Trademark of METCO, Inc., Westbury, New York, USA.
† Trademark of the Inco family of companies.

2.2. *Cathode and powder characterizations*

The three nickel powders listed in the preceding section were used to investigate the effects of powder particle size and morphology on the hydrogen evolution efficiency of plasma-sprayed cathode coatings. The powders were examined by scanning electron microscopy and their BET specific surface areas were determined. The surface morphologies of plasma-sprayed nickel cathode coatings were examined by scanning electron microscopy. Coating structures and thicknesses were determined from optical photomicrographs of polished electrode cross-sections. Both techniques were used to examine plasma-sprayed cathode coatings before and after electrochemical tests. The presence of nickel oxide in the plasma-sprayed nickel coatings was established by X-ray diffraction; its spatial distribution within the coatings was determined by electron beam microanalysis.

2.3. *Electrochemical measurements*

The electrochemical cell used for current density against overpotential measurements of sheet and screen cathodes was a straight-walled polypropylene beaker with a PTFE cover machined to a tight fit. The cell, containing 30 wt % aqueous KOH electrolyte, was maintained at a temperature of 80° C in a thermostatted water bath. A large planar nickel counterelectrode was placed about 3 cm from the test cathode. An external SCE reference electrode was connected to the cell by a Luggin probe, the tip of which was positioned near the working electrode. For testing disc electrodes in the PTFE long-term test cell, a Hg/HgO reference electrode was used. Each sheet or screen test cathode was operated at a constant current density of 200 mA cm^{-2} for 6 h. Electrode potentials were measured at several current densities from 600 to 0.5 A cm^{-2} in descending order. Disc cathodes were operated for up to 1600 h in the PTFE long-term test cell, with current density against potential measurements taken at least once each 24 h. The raw current against potential data were corrected for ohmic resistance effects using a computer method [10]. The coefficient of determination for the *iR*-free log current against potential line was generally greater than 0.99 for the

Table 1. Specific surface areas of nickel powders used to prepare cathode coatings

Powder	*Observed, BET*	*Equivalent sphere*	*Ratio*
Ni 123	0.50	0.169	3.0
56F-NS	0.17	0.022	7.7
56C-NS	0.12	0.011	10.9

Note: Specific surfaces areas are given in $m^2 g^{-1}$. The equivalent sphere specific surface areas were based on 100% dense particles with the following diameters: Ni 123, 4 μm; METCO 56F-NS, 30 μm; METCO 56C-NS, 60 μm.

current range 1–200 mA cm^{-2}, and frequently for the entire current density range of 1–600 mA cm^{-2}.

3. Results

3.1. *Morphology and composition of cathode coatings and powders*

Scanning electron microscopy showed that INCO Type 123 nickel powder, which is prepared by carbonyl decomposition, was considerably finer (roughly 4–5 μm particle diameter) than the METCO powders and covered with spiky protrusions. METCO 56F-NS nickel powder consisted of roughly spherical particles about 30 μm in diameter; METCO 56C-NS powder had a similar morphology and a particle diameter of about 60 μm. The surface features of the METCO powders indicated that they were agglomerates of finer carbonyl-decomposed nickel powder.

The BET specific surface areas of the three powders in column 2 of Table 1 were, as expected, inversely related to the powder particle diameters. If each powder species consisted of fully-dense spherical particles, their specific surface areas would have been as listed in column 3 of the table. Column 4 gives the ratio of the BET and equivalent sphere specific surface areas, i.e. the column 2 value divided by the column 3 value. As expected from its morphology, Ni 123 powder had a specific surface area considerably higher than its equivalent sphere. The data in Table 1 indicate that the two METCO powders had considerably lower measured surface areas per unit weight; however, their specific surface areas were higher relative to their equivalent spheres, indicating considerable internal surface area in the agglomerates.

Plasma-sprayed cathode coatings prepared with the three nickel powders are shown in Figs. 1 (Ni 123), 2 (56F-NS) and 3 (56C-NS). All of the coatings showed the particle deformation, flattening and interlocking characteristic of the spraying process. As can be seen from the scanning electron micrographs of Figs. 1–3, the roughnesses of the coating surfaces were inversely related to the size of the powders used to prepare them. On some areas of the two METCO powder coatings, the surface features indicated that some agglomerates may have separated during the spraying process or on impact, so that individual particles similar to Ni 123 were deposited.

The darker regions in the coating cross-sections in Figs. 1–3 indicated that the powders were partially oxidized during the spray-coating process, and that oxidation was more extensive as the particle size decreased and the powder specific surface area increased. Electron beam microanalyses confirmed that the darker regions of the coatings had higher oxygen contents than lighter regions. X-ray diffraction analyses of the coatings showed that nickel oxide was indeed present, and further that the NiO content was highest in the Ni 123 coatings and lowest in the 56C-NS coatings. To the unaided eye, cathode coatings made with Ni 123 powder were grey or black, while the coatings made with the 56F-NS and 56C-NS powders had a metallic luster.

3.2. *Current against potential behaviour*

As reported in the literature [1] and demonstrated by the data in Table 2, plasma-sprayed nickel cathode coatings greatly reduced the hydrogen evolution overpotentials of steel cathodes. The plasma-sprayed nickel cathode coatings were also much more efficient than other nickel cathodes, including nickel mesh and nickel sheet [8]. The most striking result, however, was that plasma-sprayed nickel cathode coatings evolved hydrogen much more efficiently than high surface area nickel cathode forms such as porous, sintered plaques [8] and porous, sintered coatings on steel substrates.

Among the plasma-sprayed nickel coatings made with different nickel powders, there were

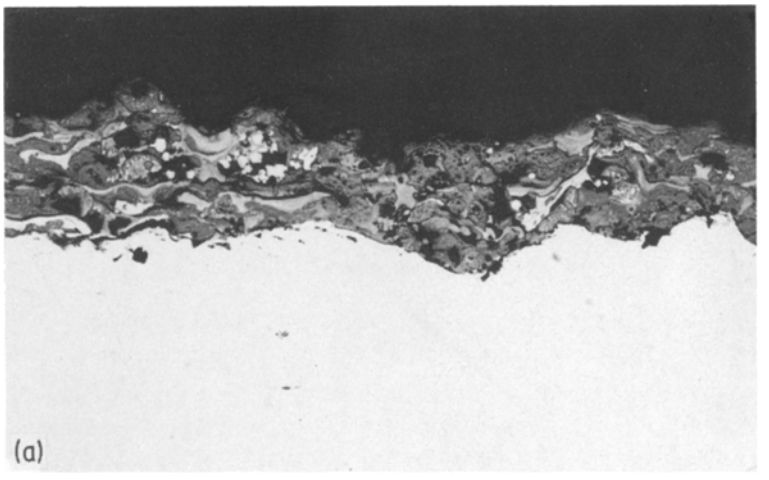

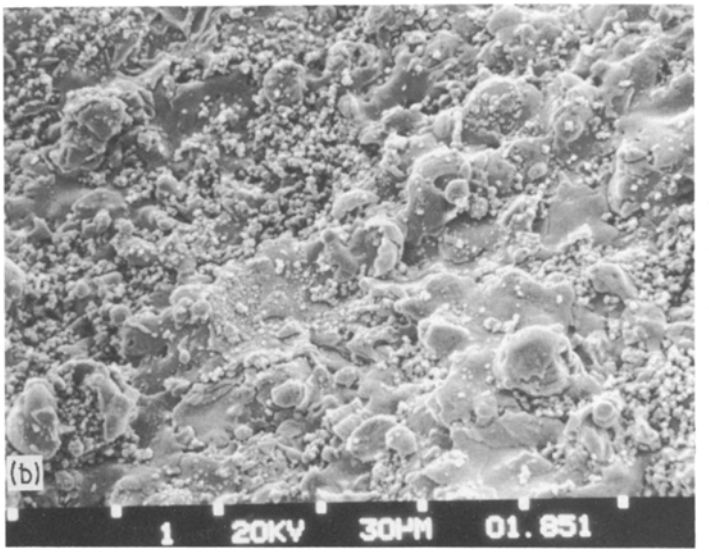

Fig. 1. Plasma-sprayed Ni 123 cathode coating. (a) Cross-section, 336 X. (b) Surface, 420 X.

systematic variations in overpotential. Table 2 shows that, at current densities typical of industrial chlor-alkali or alkaline water electrolysis cells, the plasma-sprayed coating efficiencies were in the order Ni 123 > 56F-NS > 56C-NS. Overall, there was an overpotential difference of more than 80 mV between the most- and least-efficient cathodes. This order was parallel to both the relative nickel oxide contents and the relative surface roughnesses of the three coating types.

With both morphological and chemical differences between the cathodes, the question arose whether their efficiencies were related to specific catalytic effects, or were the result of surface area differences. The present work established that the high efficiencies of plasma-sprayed nickel cathode coatings with respect to other nickel cathodes, and the relative efficiencies of the three plasma-sprayed types, were not due to observable surface area increases. Defining the cathode roughness factor as the ratio of electrochemically-active (effective) to apparent (geometric) surface area, it is obvious that the roughness factor would have to be very much higher for plasma-sprayed Ni 123 coatings, for example, than for porous, sintered Ni 123 coatings to explain the overpotential differences between them in Table 2. In fact, the sintered coatings were not only more porous than the plasma-sprayed coatings, but retained much more of the high surface morphology of the

Table 2. Hydrogen evolution overpotentials and Tafel parameters

Coating	*Substrate*	η_{H_2} (at 200 mA cm^{-2})	*b*, (mV/decade)	$10^4 i_0$, (A cm^{-2})
Plasma-sprayed Ni 123	Steel sheet	0.108–0.140	21–49	0.06–2.0
Plasma-sprayed Ni 123	Steel screen	0.102–0.136	24–44	0.13–1.9
Plasma-sprayed 56F-NS	Steel sheet	0.145–0.150	51–56	2.3 –5.1
Plasma-sprayed 56C-NS	Steel sheet	0.161–0.190	58–62	~3.5
Sintered Ni 123	Steel sheet	0.32 –0.40	130–175	1.6 –3.4
Oxidized Sintered Ni 123	Steel sheet	0.20 –0.26	60–80	0.78–1.9
None	Steel sheet	0.38 –0.40	~140	2.5 –4.0

starting powder [6]. It is also unlikely that the overpotential differences between the three types of plasma-sprayed coatings were due to the small variations in surface morphology shown in Figs. 1–3. The exchange current densities for the plasma-sprayed cathode coatings were inconsistent with a surface area interpretation of cathode efficiency. If there were no variations in reaction mechanism or electrocatalytic activity between the three coating types, the observed exchange current densities (i_0) would have been proportional to the effective cathode surface areas. Table 2 shows that observed i_0 values for Ni 123 coatings (6.2×10^{-6} to 2.0×10^{-4} A cm^{-2}) were actually lower than for 56F-NS coatings ($2.3–5.1 \times 10^{-4}$ A cm^{-2}) or 56C-NS coatings ($\sim 3.5 \times 10^{-4}$ A cm^{-2}). The higher i_0 values for the plasma-sprayed coatings were similar to those for the much less-efficient sintered coatings.

As the data in Table 2 make clear, it was the very low slopes (b) of the overpotential (η_{H_2}) against log current density (i) plots, rather than high i_0 values, which resulted in the low overpotentials of plasma-sprayed nickel cathode coatings. This was particularly true for the Ni 123 coatings, for which b values were distributed rather evenly over the range 21–49 mV/decade for sheet cathodes and 24–44 mV/decade for screen cathodes. The η_{H_2} against log i slopes for 56F-NS coatings were higher (51–56 mV/decade) and for 56C-NS coatings were slightly higher still (58–62 mV/decade). All of these values were far below the Tafel slopes usually reported for smooth or porous nickel cathodes in alkaline electrolytes [8]. Thus, it was concluded that the high efficiencies of plasma-sprayed nickel cathode coatings were due to changes in electrode kinetics induced by oxidation, rather than high surface area. Available evidence indicates that surface oxides persist on nickel cathodes even under conditions of hydrogen evolution [11]. Yoshida and Shiroki [5] postulated that the high efficiency of oxidized nickel cathodes was due to restructuring of the nickel surface by oxidation, and that the restructured nickel skeleton was preserved under mild reduction conditions, such as in electrochemical hydrogen evolution or gaseous H_2 reduction at low temperatures. As discussed later, however, electrochemical and thermal reductions were not found to be equivalent in the present work.

The main feature which differentiated the three types of plasma-sprayed nickel coatings from one another, and all of them from sintered nickel coatings, was their nickel oxide content. As shown earlier, the efficiencies of the plasma-sprayed nickel coatings increased with the degree of oxidation, and were all much higher than the efficiencies of unoxidized nickel cathodes. The critical role of the oxide was confirmed with the following two experiments.

When porous, sintered nickel cathode coatings were thermally oxidized, their hydrogen evolution overpotentials dropped markedly (Table 2). Similar effects have also been observed on other nickel cathode forms [5]. The overpotential differences between unoxidized and oxidized sintered nickel coatings were not due to morphological changes observable by scanning electron microscopy. On the basis of cathode surface area, the oxidized sintered coatings should have been more efficient than plasma-sprayed coatings. However, the constant temperature oxidation of the former did not duplicate the rapid, highly non-equilibrium oxidation conditions of the plasma-spraying process, in which temperatures can exceed 3000° C for brief intervals [12]. In the second experiment,

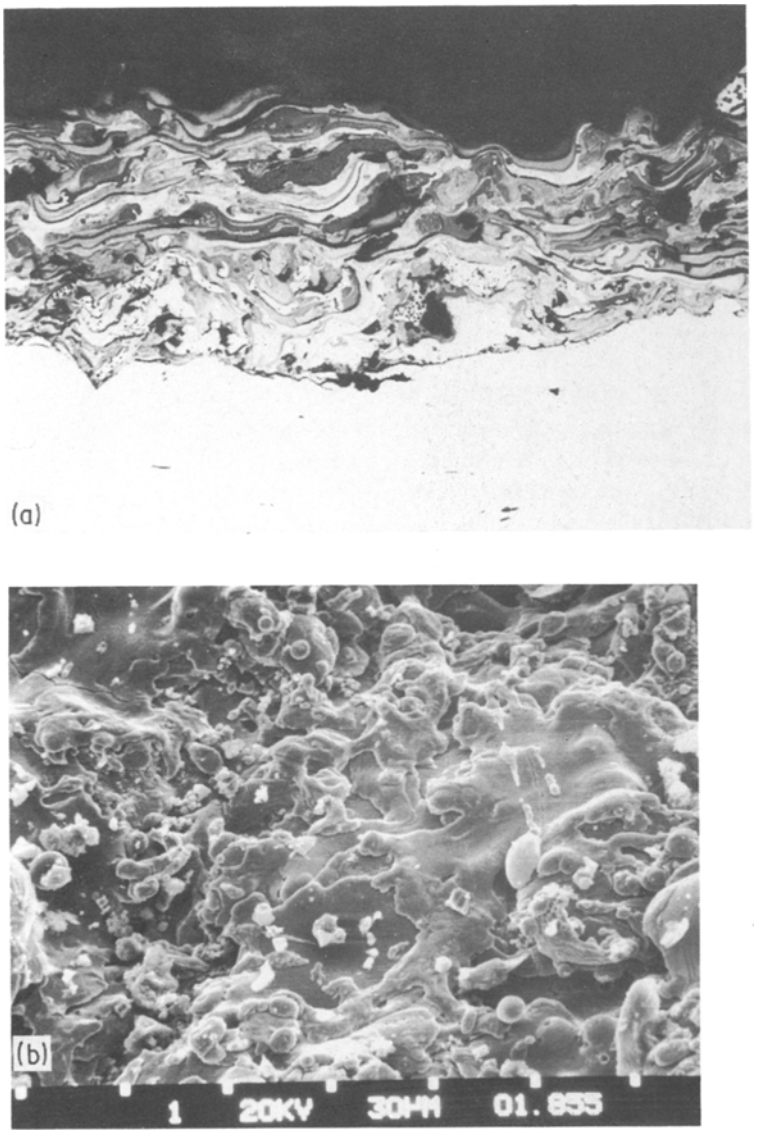

Fig. 2. Plasma-sprayed METCO 56F-NS cathode coating. (a) Cross-section, 336 X. (b) Surface, 420 X.

both sheet and screen cathodes with plasma-sprayed Ni 123 coatings were reduced under flowing hydrogen at temperatures from 200 to 500° C. Figure 4 shows the current against potential behaviour of the sheet cathodes: the results for screen cathodes were essentially similar. Even at the lowest reduction temperature, some of the high efficiency of the plasma-sprayed coating was lost. Furthermore, as Fig. 4 makes clear, the efficiency loss could be attributed directly to an increase in the η_{H_2} against log i slope from the normal plasma-sprayed Ni 123 value to that characteristic of other nickel cathodes. Optical microscopy of coating cross-sections showed that the dark, oxidized regions were absent in all of the reduced coatings, in which the oxide level had dropped below the limits of detection by electron beam microanalysis. The overpotential increase at the reduced coatings could not be attributed to a decrease in cathode surface area observable by scanning electron microscopy. The coatings reduced at 200° C were virtually identical in morphology to unreduced standards; some coating densification was observed at the higher reduction temperatures, but the effect was small. These results do not agree with those of Yoshida and

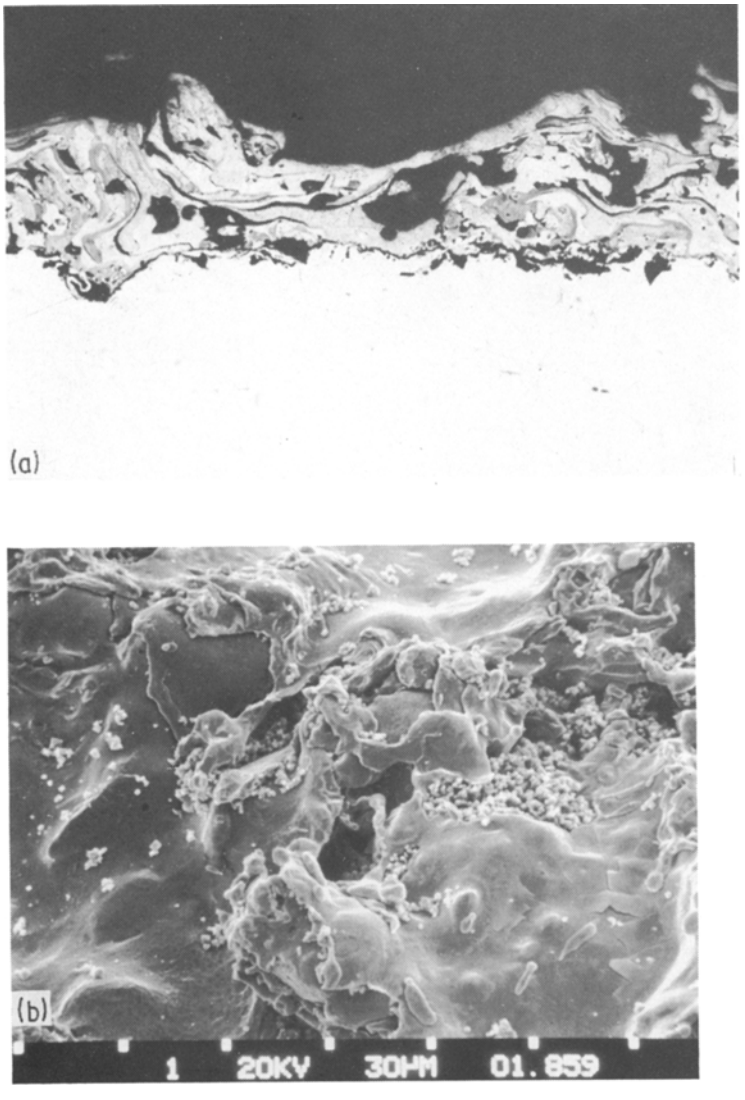

Fig. 3. Plasma-sprayed METCO 56C-NS cathode coating. (a) Cross-section, 336 X. (b) Surface, 420 X.

Shiroki [5], who found that oxidized nickel cathodes reduced under hydrogen at 80–300° C were highly efficient.

3.2. *Ni(OH)$_2$ impregnation*

Hydrogen evolution overpotentials at porous, sintered nickel cathodes have been reduced significantly by impregnation with nickel hydroxide [8]. In the present work, this technique was applied to plasma-sprayed Ni 123 cathode coatings. However, because of the much lower porosity of the plasma-sprayed coatings, the $Ni(OH)_2$ loadings per unit of geometric surface were kept lower. A linear relationship was obtained between the amount of $Ni(OH)_2$ precipitated and the charge passed during the precipitation process, with a proportionality constant of about 1400 $C\,g^{-1}$. Scanning electron microscopy showed that the surface recesses and voids of the plasma-sprayed coatings were plugged with $Ni(OH)_2$ at loadings of only 0.4–0.5 $mg\,cm^{-2}$. A cracked, 'mud flats' appearance characteristic of $Ni(OH)_2$ surface coverage was evident at $Ni(OH)_2$ loadings of about 0.6 $mg\,cm^{-2}$; still higher loadings produced a fluffy outer layer of $Ni(OH)_2$ on the denser, cracked underlayer.

The maximum overpotential reductions resulting from $Ni(OH)_2$ impregnation were small (about 25 mV), giving hydrogen evolution overpotentials of 95–105 mV at a current density of

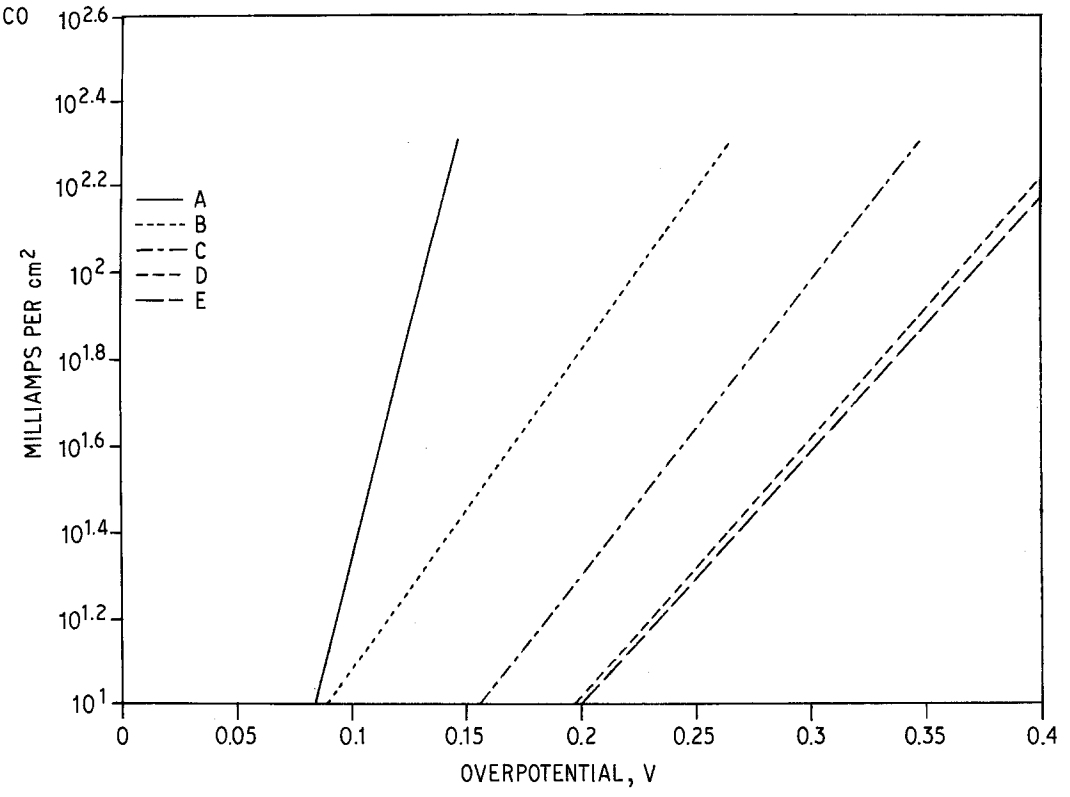

Fig. 4. Current against potential data for plasma-sprayed Ni 123 cathode coatings reduced under flowing hydrogen for 30 min. Curve A, no reduction (as sprayed); curve B, 200° C; curve C, 300° C; curve D, 400° C, curve E, 500° C.

200 mA cm^{-2}. This maximum improvement was reached at $Ni(OH)_2$ loadings of about 0.4 mg cm^{-2}, i.e. near the onset of complete $Ni(OH)_2$ surface coverage, and persisted at higher loadings. The small differences in overpotential between the NiO and $Ni(OH)_2$ (which may be thought of as the hydrated from of NiO) indicate that both may produce the same cathode surface composition under cathodic polarization.

3.4. *Long-term tests*

Three cathodes with plasma-sprayed Ni 123 coatings were operated for 1600 h. During the early phases of operation, their overpotentials were comparable to those obtained in 6 h tests. Each cathode showed a nearly linear 0.02 mV h^{-1} increase in overpotential with time. Whether this was due to loss of electrocatalytic activity or to metallic impurity pickup, a mechanism of cathode deactivation which has been discussed elsewhere [5, 13], is not known. None of the cathodes showed structural failure, i.e. coating separation or deterioration, during the tests. One noteworthy result was the persistence of the nickel oxide in the coatings at the conclusion of electrolysis. Optical microscopy showed that the dark, oxidized regions of the coatings were still present. Any nickel oxide reduction which occurred was too restricted to be seen by microscopic examination. This result is consistent with the earlier-mentioned evidence [11] that surface oxides persist during hydrogen evolution and that thermal and electrochemical reductions of oxidized nickel cathodes are not equivalent.

Acknowledgements

The author thanks the following for their contributions to the present work. Plasma-sprayed nickel cathode coatings were prepared by R. K. Wilson and N. Sorice. Porous, sintered nickel cathode coatings were prepared by G. Hawks. Electrochemical measurements were made by A. M. Rapun. Scanning electron microscopy and electron

microprobe analysis were carried out with the help of M. Santana and F. Veltry.

References

[1] T. G. Coker and S. D. Argade, US Patent No. 4049 841, September 20 (1977).
[2] C. N. Welch and J. O. Snodgrass, US Patent No. 4248 679, February 3 (1981).
[3] C. N. Welch and J. O. Snodgrass, US Patent No. 4251 478, February 17 (1981).
[4] J. M. McIntyre and D. L. Caldwell, US Patent No. 4279 709, July 21 (1981).
[5] M. Yoshida and H. Shiroki, European Patent Application No. 80108172.0, December 23 (1980).
[6] D. E. Hall, *J. Electrochem. Soc.* **128** (1981) 740.
[7] *Idem, ibid.* **129** (1982) 310.
[8] A. J. Appleby, G. Crepy and J. Jacquelin, *Int. J. Hydrogen Energy* **3** (1978) 21.
[9] E. J. McHenry, *Electrochem. Technol.* **5** (1967) 275.
[10] R. L. LeRoy, M. B. I. Janjua, R. Renaud and U. Leuenberger, *J. Electrochem. Soc.* **126** (1979) 1674.
[11] A. P. Brown, M. Krumpelt, R. O. Loutfy and N. P. Yao, *ibid.* **129** (1982) 2481.
[12] S. Safai, in 'Treatise on Materials Science and Technology', Vol. 20, edited by H. Herman, Academic Press, New York (1981).
[13] L. A. Avaca, A. Carubelli and E. R. Gonzalez, Proceedings of the 3rd World Hydrogen Energy Conference, Tokyo, Japan, 23–26 June, 1980.